Electric Lines of Force of an Electrically Small Dipole-Loop Antenna Array

P. L. Overfelt

***Abstract*— The electric lines of force of an electrically small dipole-loop antenna array have been determined analytically for both the near- and far-fields of the array. It has been found that the behavior of the families of electric contours are dependent upon a coupling parameter, which is the ratio of the loop and dipole sizes and currents. This parameter also controls the appearance (or not) and position of the points of equilibrium for the radiated field when analyzed in a real phase plane. The electric lines of force of the dipole-loop array exhibit increased directivity in the plane of the array when the coupling parameter is purely real, indicating that the respective dipole and loop currents must be in phase quadrature for this effect to occur.**

***Index Terms*— Antenna arrays.**

I. Introduction

ELECTRICALLY small antennas are often necessary for missile systems due to limited space requirements or reduction in radar cross section. For some systems, even at UHF and VHF frequencies, the antenna can be isolated as the single most heavy and bulky component [1]. Performance penalties in bandwidth and efficiency occur from reduction in size resulting in serious problems for the system as a whole. Such performance penalties must be absorbed into the overall system performance with subsequent poor reception in low signal regions. Matching techniques can be used to increase antenna performance but a drop in total efficiency is still incurred.

Several methods to counteract the above problems have been considered. For electrically small antennas/antenna arrays with radiation resistance lower than the ohmic resistance of their radiating elements and that include feed and matching networks, one such solution has been to obtain higher efficiencies when all components are composed of high-temperature superconducting (HTS) materials [2]–[4]. However, this replacement of normal conductors with HTS components can only partially compensate for the drop in efficiency upon size reduction. Thus, it is advantageous to obtain as large an efficiency as possible from a given antenna by other means first.

A very different method has been investigated for some years and proposes using judicious combinations of electric and magnetic multipole sources [5]–[9] to attempt to exceed the small antenna limitations derived by Chu [10], Harrington [11], and Wheeler [12], [13]. The simplest example of this class of antennas—an electric-dipole magnetic-loop array—is the subject of the present work. A complete analysis (including moment method (MM) modeling) has been published elsewhere [14], [15]. An independent verification of the numerical results in [14] has been performed also [16]. A prototype array with matching networks has been built and is currently being tested [17], [18]. Its performance will be discussed in a future work. For now, we are attempting to understand the differences in an electromagnetic field sense between an array of this type and a single-element antenna such as a dipole. One way in which to do this is to determine the electric lines of force in both the near- and far-field regions of the array. Contour plots of these lines of force over time give a physical picture of how such an antenna radiates.

Since the mathematics is much simpler, the electric lines of force in the far field are discussed initially in Section II. The integral curves of the coupled ordinary differential equations (ODE's), which occur as a result of having six nonzero electric and magnetic field components, are determined and their significance is interpreted geometrically. A phase plane analysis of these far-field solutions is considered in Section III. The near-field equations of the lines of force are derived in Section IV. In Section V, contour plots of the electric lines of force are shown and discussed. Section VI contains the conclusions.

II. Far-Field Analysis

The geometry of the harmonically oscillating electric-dipole magnetic-loop array antenna is shown in Fig. 1. The dipole with current I_d and length ℓ runs along the $\hat{z}$ axis as usual, while the loop surrounds the dipole without touching it and the plane of the loop is the yz plane. Since we are interested in antenna arrays that are electrically small, we use the infinitesimal model for both elements of the array and replace the loop with an equivalent magnetic dipole along the $\hat{x}$ axis with equivalent magnetic current I_m and length ℓ_m. The electric field components are given in [15].

For this geometry, all three electric field components (and magnetic field components) are nonzero and immediately it is obvious that the E_r component is due to the dipole alone, the E_ϕ component is due to the loop alone, and only E_θ contains contributions from both elements.

The electric lines of force are given by [19] and [20] (in standard spherical coordinates)

$$\frac{d\theta}{dr} = \frac{E_\theta}{rE_r}; \quad \frac{d\phi}{dr} = \frac{E_\phi}{E_r r \sin\theta} \tag{1}$$

Manuscript received April 4, 1996; revised September 15, 1997.

The author is with the Research and Technology Group, Naval Air Warfare Center Weapons Division, China Lake, CA 93555 USA.

Publisher Item Identifier S 0018-926X(98)01498-7.

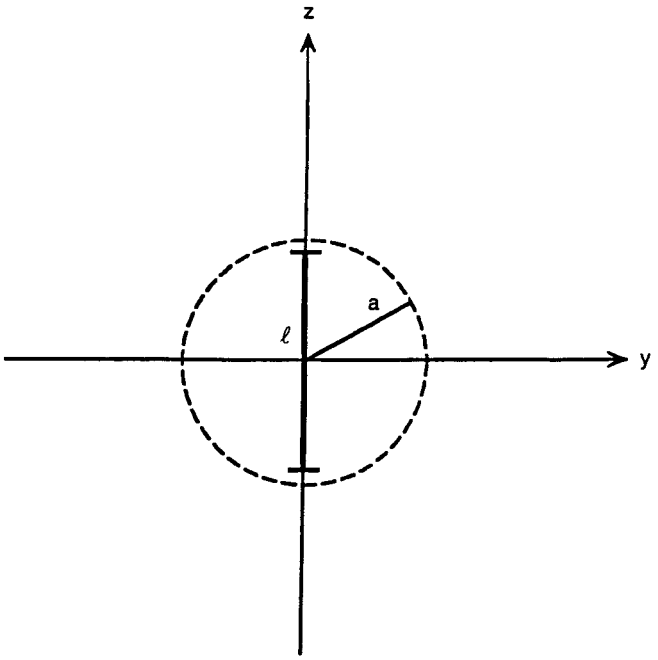

Fig. 1. Dipole-loop array geometry.

which are two simultaneous coupled ODE's. Equation (1) expresses the fact that an element $\vec{d\ell}$ of a line of force is parallel to the electric field vector. Thus, the components of $\vec{d\ell} = dr\,\hat{r} + rd\theta\,\hat{\theta} + r\sin\theta\,d\phi\,\hat{\phi}$ are proportional to the components of $\vec{E} = E_r\hat{r} + E_\theta\hat{\theta} + E_\phi\hat{\phi}$. This relationship gives the set of equations in [21, eq. (1)]. Since E_r, E_θ, and E_ϕ are each functions of r, θ, and ϕ, they generate a similar system of curves, any one of which can be considered as the trajectory of a moving point that continuously alters its direction of motion.

For geometrically simpler antennas, such as the small electric dipole alone or the small magnetic loop alone, usually at least one of the electric field components is zero and, thus, (1) reduces to only one equation. In the case of the dipole-loop array, one is faced with two simultaneous coupled ODE's. The electromagnetic field components are based on *a priori* known constant currents in an infinitesimal model and are exact (to within these limits) with respect to both the near and far fields.

In a far field analysis, if the $1/r^3$ term in E_θ is neglected, a tremendous simplification is introduced into (1). Assuming that $x = ikr$ for convenience in (1), the first equation in (1) can be written as

$$\cos\theta\frac{d\theta}{dx} = \alpha\sin\theta + \beta\sin\phi \tag{2a}$$

while the second equation in (1) becomes

$$\frac{d\phi}{dx} = \frac{\beta\cos\phi}{\sin\theta} \tag{2b}$$

where $\alpha = \frac{1}{2}$, and $\beta = \frac{I_m\ell_m}{2\eta I_d\ell_d}$. α and β are ratios of the constants appearing in the field components [15]. Thus, β is the ratio of the loop and dipole equivalent lengths and currents. It is a constant for a given geometry and excitation with *a priori* specified constant current distributions.

Further simplification of (2) occurs via appropriate variable substitutions. Setting

$$u = \sin\theta(x) \quad \text{and} \quad \xi = \sin\phi(x) \tag{3}$$

(after a good deal of algebra) we obtain the far-field solutions for the electric lines of force, i.e.,

$$C_1 = (u^2 + 4\beta u\xi + 4\beta^2)e^{-x} = f(r,\theta,\phi) \tag{4a}$$

and

$$C_2 = -4\beta(2\beta + u\xi)e^{-x/2} = g(r,\theta,\phi). \tag{4b}$$

These functions f and g represent the integral curves of (1) in the far field [21], [22]. A particular pair of values (C_1, C_2) defines one curve in (r,θ,ϕ) space, which is the intersection of the surfaces f = constant and g = constant. Each surface is thus swept out by a one-parameter family of integral curves [15], [22]. C_1 and C_2 are general constants of integration and β can be rewritten in terms of the actual loop parameters as

$$\beta = \frac{i\pi}{2}\frac{(ka)^2}{k\ell}\left|\frac{I_\ell}{I_d}\right|e^{i(\phi_2-\phi_1)} \tag{5}$$

where a is the loop radius, I_ℓ is the loop current, and I_d is the dipole current. We have written the currents on the loop and dipole in the polar form $I_\ell = |I_\ell|e^{i\phi_1}$, $I_d = |I_d|e^{i\phi_2}$. Note that in general, β is complex. However, we are mainly interested in two cases: 1) when $\phi_1 = \phi_2$, the currents are in phase, β is pure imaginary, and thus $\beta^2 < 0$ and 2) when $\phi_1 - \phi_2 = \frac{\pi}{2}$ and the currents are in phase quadrature, then β is pure real, and $\beta^2 > 0$. In each of these cases, β can be either negative or positive depending on whether the dipole phase leads (or lags) the loop phase, respectively.

At this point, we consider the electric lines of force of the small electric dipole alone. An excellent analysis was given years ago by Lorraine and Corson [23]. In this case, E_ϕ is zero and, thus, only one ordinary differential equation must be solved. In the far field for $kr \gg 1$ [23] and using our notation we have

$$C_1 = \sin^2\theta e^{-(ikr - i\omega t)} \tag{6}$$

Comparing (6) with (4a) when no loop is present, both β and C_2 in (4) must equal zero and the equation for C_2 vanishes as it should. It is important to note that for the electric dipole alone as given in (6), the constant contains the dipole length and current, but since it does not have to be related back to an absolute standard or another element, C_1 is simply a scaling parameter which varies from one line of force to the next. The situation for the dipole-loop array is very different. In this case, C_1 and C_2 are both parameters that vary from one line of force to the next, but they do not contain the currents and sizes of the array elements and they do not simply scale. The parameter β contains this information explicitly rather than having it embedded in C_1 or C_2.

III. Far-Field Lines of Force in the Phase Plane

A nonlinear variable transformation can be used to put (2) into extremely simple form. Using $P = u\xi = \sin\theta\sin\phi$ and $Q = u^2 = \sin^2\theta$ in (2), the coupled ODE's in the far field

reduce to an inhomogeneous constant coefficient first-order system. Using $x = ikr$ while P, Q, and β are complex in general, it is obvious that

$$P(x) = -\frac{C_2}{4\beta}e^{x/2} - 2\beta \tag{7a}$$

and

$$Q(x) = C_1 e^{x} + C_2 e^{x/2} + 4\beta^2. \tag{7b}$$

Viewing the PQ plane (or, alternately, the $\theta\phi$ plane) as the phase plane of the system [15], [24] and writing $\beta = \beta_1 + i\beta_2$, an equilibrium point of the system occurs wherever $\frac{d(\mathrm{Re}[P])}{dr} = \frac{d(\mathrm{Re}[Q])}{dr} = 0$, i.e., where $\mathrm{Re}[P] = -2\beta_1$ and $\mathrm{Re}[Q] = 4(\beta_1^2 - \beta_2^2)$. Thus, in the real $\theta\phi$ plane, an equilibrium point occurs at

$$\sin\theta = \pm 2\left(\beta_1^2 - \beta_2^2\right)^{1/2} \tag{8}$$

and

$$\sin\phi = \frac{-\beta_1}{\pm\left(\beta_1^2 - \beta_2^2\right)^{1/2}}. \tag{9}$$

From (8) and (9), several special cases are apparent. If β is pure real, i.e., $\beta_2 = 0$, then an equilibrium point occurs at $\theta = \sin^{-1}(2\beta_1)$, $\phi = \frac{3\pi}{2}$ and also at $\theta = \sin^{-1}(-2\beta_1)$, $\phi = \frac{\pi}{2}$. Immediately for this case, θ remains real only when $|\beta_1| \leq \frac{1}{2}$. If $|\beta_1| > \frac{1}{2}$, there is no equilibrium value for θ in the purely real phase plane since in this instance, θ would be forced to become complex in order for a solution to the above to exist.

Alternatively, if β is pure imaginary, i.e., $\beta_1 = 0$, then $\sin\phi = 0$ but $\sin\theta = \pm i2\beta_2$ is the only possible solution in θ. Thus, no equilibrium point is possible in the purely real phase plane for this case.

In general, if both β_1 and β_2 are nonzero, as long as $\beta_2 < \beta_1$, (9) may be satisfied and from (8), we have the condition that $0 \leq (\beta_1^2 - \beta_2^2)^{1/2} \leq \frac{1}{2}$ must always hold if θ and ϕ are to remain real.

Previously, we had determined via both analysis and MM modeling that when the loop current is driven in phase quadrature to the dipole current, an increased directivity effect is seen [14]. This corresponds to the case where $\beta_2 = 0$ and from (5) $\beta = \beta_1 = \frac{\pi}{2}\frac{(ka)^2|I_\ell|}{(k\ell)|I_d|}$ when $\phi_1 - \phi_2 = \frac{\pi}{2}$.

Also previously, we had determined that when the loop and dipole currents were driven in phase, then the array radiates exactly as if each element stood alone [14]. This is the case where β is pure imaginary. In this instance, no real equilibrium point exists for any value of β_2.

This is extremely interesting in the sense that β, the ratio of the array element sizes and currents, controls the points of equilibrium in the phase plane associated with the far-field electric lines of force. Thus, changing the geometry and/or the excitation such that β_1 and β_2 change will result in different equilibrium points or none at all in the real phase plane.

IV. Near-Field Analysis

Returning to the electric field components in [15], it is possible in the case of the dipole-loop array to obtain an analytically soluble system of ODE's for the electric lines of force in the near field of the antenna. This is by no means the usual case. It is usually impossible to obtain analytic near-field solutions for any geometries other than very simple single-element antennas. Keeping the $1/r^3$ term in the E_θ component in (1) and using the variable transformation in Section III, (1) becomes

$$\frac{dP}{dx} = \frac{1}{2}w(x)P + \beta \tag{10a}$$

and

$$\frac{dQ}{dx} = w(x)Q + 2\beta\, P \tag{10b}$$

where $w(x)$ is a ratio of two polynomials, i.e., $w(x) = \frac{x^2+x+1}{x^2+x} = 1 + \frac{1}{(x^2+x)}$. Obviously $w(x)$ approaches one as $|x|$ becomes greater than one. Without detail [15], we find that

$$C_1 = Q\left(\frac{x+1}{x}\right)e^{-x} - 2\beta I(x)Pe^{-x/2}\sqrt{\frac{x+1}{x}} + \beta^2 I^2(x) \tag{11a}$$

and

$$C_2 = -4\beta\left[Pe^{-x/2}\sqrt{\frac{x+1}{x}} - \beta I(x)\right] \tag{11b}$$

with $e^{i\omega t}$ understood and where $I(x)$ is given by either [15]

$$I(x) = \sum_{n=0}^{\infty}\binom{1/2}{n}2^{n+1/2}\,\gamma\left(n+\frac{1}{2};\frac{x}{2}\right),\ |x|<1 \tag{12}$$

or

$$I(x) = -2e^{-x/2} + \sum_{n=1}^{\infty}\binom{1/2}{n}2^{(1-n)}\,\Gamma\left(1-n;\frac{x}{2}\right),\quad |x|>1. \tag{13}$$

Provided the appropriate series expansions are used for $I(x)$ in the appropriate regions, (11) are the exact solutions for contours of the electric lines of force of the electrically small dipole-loop array everywhere in space (excluding $|x| = 0$).

V. Electric Lines of Force

By taking the real parts of (11), we can plot the contours C_1 and C_2 obtained from solving the differential equations for the electric lines of force. Figs. 2–9 each consist of four graphs for varying values of ωt, i.e., $\omega t = 0$ in the top-left plot, $\omega t = \pi/2$ in the top-right plot, $\omega t = \pi$ in the bottom-left plot, and $\omega t = 3\pi/2$ in the bottom-right plot. Each of these figures shows how the electric lines of force are changing in time in a given plane where $\beta = \beta_1 + i\beta_2$ is varied. The reader is cautioned that the portions of the contours for each of Figs. 2–9 in the region $kr < 1$ are not as accurate as those in the region where $kr > 1$. Fig. 2 consists of four plots in the xz plane of the C_1 contours for the four different values of ωt mentioned above with the coupling parameter β set to zero. Since β is zero, there is no contribution to (11a) from the loop and, thus, the lines of force in this figure are identical to those for a small electric dipole radiating alone. Fig. 2 can be compared to Fig. 9 [23]. Fig. 2 is mainly for the reader's convenience so that the electric dipole case can be easily

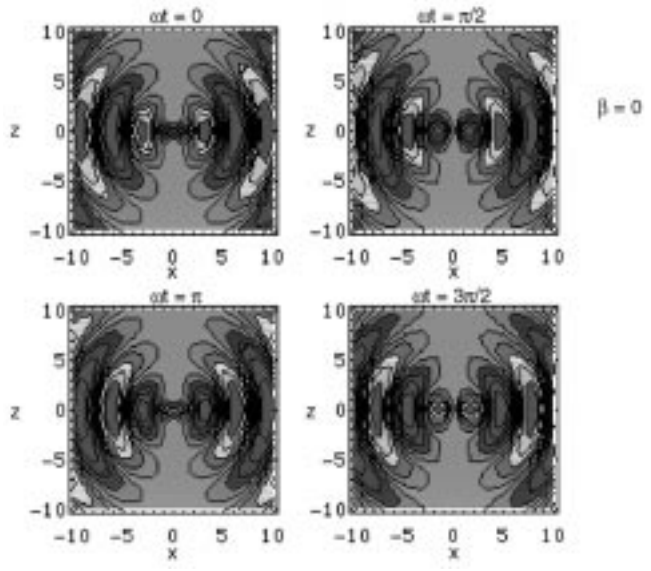

Fig. 2. Electric lines of force C_1 in the xz plane, $y = 0$, $\beta = 0$ for $\omega t = 0,\ \pi/2,\ \pi,\ 3\pi/2$.

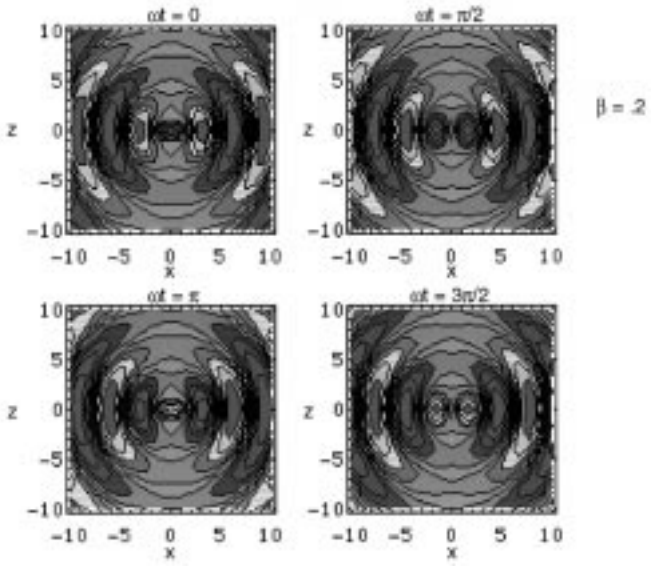

Fig. 3. Electric lines of force C_1 in the xz plane, $y = 0$, $\beta = 0.2$ for $\omega t = 0,\ \pi/2,\ \pi,\ 3\pi/2$.

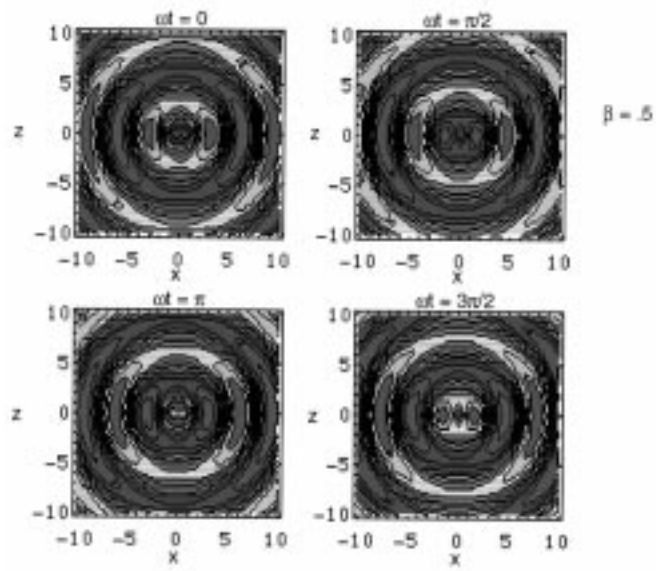

Fig. 4. Electric lines of force C_1 in the xz plane, $y = 0$, $\beta = 0.5$ for $\omega t = 0,\ \pi/2,\ \pi,\ 3\pi/2$.

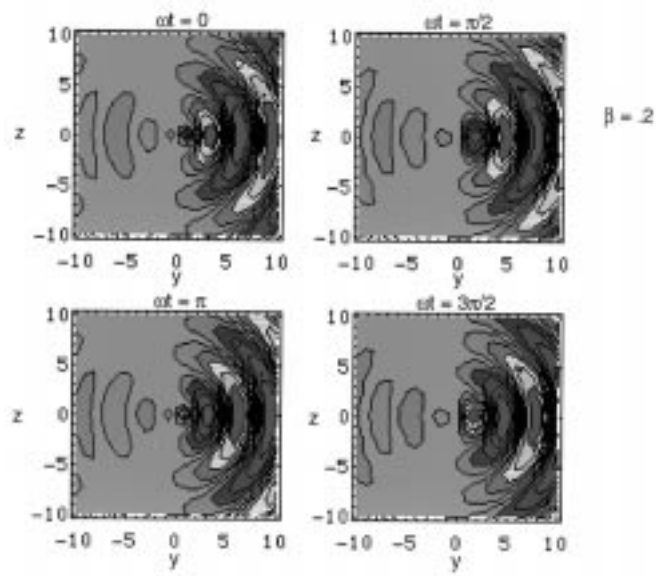

Fig. 5. Electric lines of force C_1 in the yz plane, $x = 0$, $\beta = 0.2$ for $\omega t = 0,\ \pi/2,\ \pi,\ 3\pi/2$.

compared to the succeeding array cases when β is nonzero. In Fig. 3 the C_1 contours have been plotted in the xz plane with $\beta_1 = 0.2$, $\beta_2 = 0$, and β is purely real. As β_1 increases, the contribution to the lines of force from the loop increases. Thus, certain lines of force look circular, meeting at the top and bottom of each plot along $x = 0$. This is reasonable if we recall that for a small loop alone, the electric lines of force are concentric circles in the plane of the loop. In Fig. 4, as β_1 is increased further to 0.5 with $\beta_2 = 0$, the number of circular looking contours that meet at the top and bottom of the plots for different ωt has greatly increased, while the number of electric dipole-like contours is much reduced. In Fig. 5 the C_1 contours are plotted in the yz plane with $x = 0$ and $\beta_1 = 0.2$, $\beta_2 = 0$. In this plane, the C_1 contours are asymmetric when the real part of β is nonzero, resulting in lines of force that add constructively in the positive y direction and mostly cancel in the $-y$ direction. This is the plane in which previously an increased directivity effect was predicted for the dipole-loop array provided β is purely real, implying that the currents on the dipole and loop must be in phase quadrature [14]. In Fig. 6, we show a set of four plots in the xz plane where $\beta_1 = 0$ and $\beta_2 = 0.2$. These plots are quite similar to the electric dipole plots in Fig. 2 when $\beta = 0$, thus corroborating the result in [14] that the dipole-loop array radiates like a dipole alone when the respective currents on the loop and dipole are in phase and β is pure imaginary.

Figs. 7–9 show the C_2 contours determined by taking the real part of (11b). This family of contours never appears for the dipole alone. Fig. 7 shows the C_2 contours in the xz plane

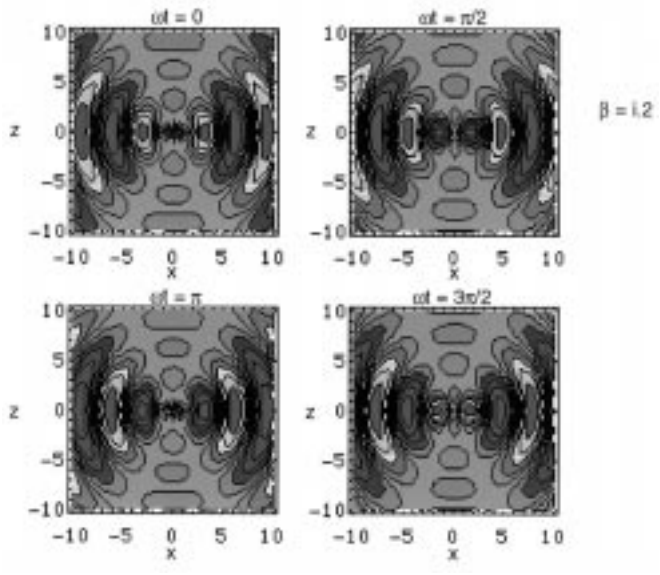

Fig. 6. Electric lines of force C_1 in the xz plane, $y = 0$, $\beta = 0.2i$ for $\omega t = 0,\ \pi/2,\ \pi,\ \pi p/2$.

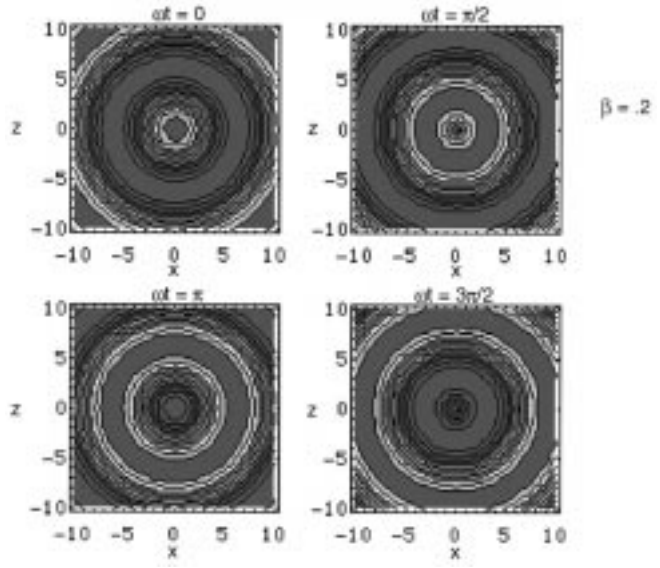

Fig. 7. Electric lines of force C_2 in the xz plane, $y = 0$, $\beta = 0.2$ for $\omega t = 0,\ \pi/2,\ \pi,\ 3\pi/2$.

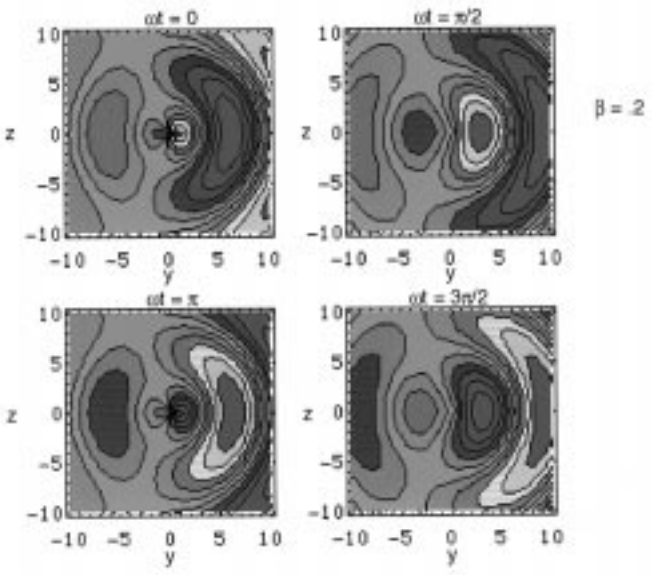

Fig. 8. Electric lines of force C_2 in the yz plane, $x = 0$, $\beta = 0.2$ for $\omega t = 0,\ \pi/2,\ \pi,\ 3\pi/2$.

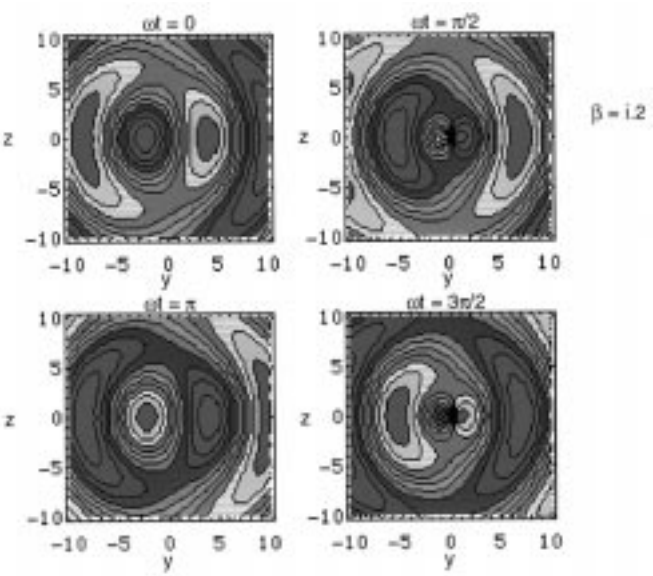

Fig. 9. Electric lines of force C_2 in the yz plane, $x = 0$, $\beta = 0.2i$ for $\omega t = 0,\ \pi/2,\ \pi,\ 3\pi/2$.

with $y = 0$ and $\beta_1 = 0.2$, $\beta_2 = 0$. These are just concentric circles since for any case in which $y = 0$, $P = 0$ also and, thus, C_2 is simply equal to the product of a constant and $\mathrm{Exp}[-i(kr - \omega t)]$. Thus, the C_2 contours in the xz plane where $y = 0$ are always concentric circles regardless of the values of β_1 and β_2. Fig. 8 shows the C_2 contours in the yz plane with $x = 0$. The C_2 contours are asymmetric in this plane, adding constructively along the $+y$ direction and mostly canceling along the $-y$ direction just as do the C_1 contours in this plane. Again $\beta_1 = 0.2$, $\beta_2 = 0$ as before, but although the value of β_1 indicates a substantial contribution from the loop, these lines of force are essentially electric dipole-like contours in this plane. In Fig. 9, we consider the pure imaginary β case for the C_2 contours. In the yz plane with $\beta_1 = 0$, $\beta_2 = 0.2$, the C_2 contours are asymmetric and exhibit a combination of both dipole and loop behavior. Though the curves are asymmetric they are not particularly directional in this case, which is what we would expect since β is pure imaginary and, thus, the currents of the dipole and loop are in phase.

VI. Conclusion

The electric lines of force of an electrically small dipole-loop antenna array have been determined analytically for both the near- and far-fields of the array. It has also been found that the behavior of the families of electric contours C_1 and C_2 are dependent upon a coupling parameter β, which is the ratio of the loop and dipole sizes and currents. The parameter β also controls the appearance (or not) and position of any points of equilibrium for the radiated field when analyzed in

a real phase plane determined by P and Q or θ and ϕ. The electric lines of force of the dipole-loop array exhibit increased directivity in the yz plane when $x = 0$ provided β is purely real, indicating that the respective dipole and loop currents must be in phase quadrature.

ACKNOWLEDGMENT

The author would like to thank D. J. White of Sverdrup, Inc., Ridgecrest, CA, and D. R. Bowling of the Naval Air Warfare Center Weapons Division, China Lake, CA, for a number of helpful technical discussions. The author would also like to thank Dr. C. Kenney of the University of California, Santa Barbara, for several numerical suggestions.

REFERENCES

[1] K. Fujimoto, A. Henderson, K. Hirasawa, and J. R. James, *Small Antennas*. New York: Wiley, 1987.
[2] S. K. Khamas, G. G. Cook, S. P. Kingsley, R. C. Woods, and N. M. Alford, "Investigation of the enhanced efficiencies of small superconducting loop antennas," *J. Appl. Phys.*, vol. 74, p. 2914, 1993.
[3] G. G. Cook, S. K. Khamas, D. R. Bowling, P. L. Overfelt, and L. Hageman, "Predictions of the efficiencies of superconducting small antennas above lossy groundplanes using a Sommerfeld integral technique," *J. Appl. Phys.*, vol. 76, p. 1266, 1994.
[4] A. P. Pischke and H. Chaloupka, "Electrically small superconducting planar radiating elements for arrays," in *22nd Eur. Microwave Conf. Proc.*, Helsinki, Finland, 1992.
[5] D. M. Grimes, "Quantum theory: The classical theory of nonlinear electromagnetics," *Phys. D*, vol. 32, p. 1, 1988.
[6] ——, "Quantum theory and classical nonlinear electronics," *Phys. D*, vol. 20, p. 285, 1986.
[7] C. A. Grimes and D. M. Grimes, "A small antenna with aerospace application," in *Aerosp. Appl. Conf. Dig.*, Crested Butte, CO, Feb. 1991, no. 3, pp. 1–10 (Session II).
[8] D. M. Grimes and C. A. Grimes, "Bandwidth and Q of antennas radiating TE and TM modes," *IEEE Trans. Electromagn. Compat.*, vol. 37, p. 217, May 1995.
[9] C. A. Grimes and D. M. Grimes, "Small antenna configurations: Implementation promises and problems," in *IEEE Int. Symp. Electromagn. Compat. Symp. Rec.*, Aug. 1995, pp. 92–96.
[10] L. J. Chu, "Physical limitations on omnidirectional antennas," *J. Appl. Phys.*, vol. 19, p. 1163, 1948.
[11] R. F. Harrington, "Effect of antenna size on gain, bandwidth, and efficiency," *J. Res. Nat. Bur. Stand.*, vol. 64D, p. 1, 1960.
[12] H. A. Wheeler, "Fundamental limitations of small antennas," *Proc. IRE*, vol. 35, p. 1479, 1947.
[13] ——, "The radiansphere around a small antenna," in *Proc. IRE*, vol. 47, p. 1325, 1959.
[14] P. L. Overfelt, D. R. Bowling, and D. J. White, "A collocated magnetic loop, electric dipole array antenna (preliminary results)," NAWCWPNS Tech. Pub. 8212, China Lake, CA, Sept. 1994.
[15] P. L. Overfelt, "Electric lines of force of an electrically small mixed mode array antenna," NAWCWPNS Tech. Pub. 8372, China Lake, CA, Oct. 1997.
[16] J. S. McLean, "The application of the method of moments to the analysis of electrically small 'compound' antennas," in *IEEE Int. Symp. Electromagn. Compat. Symp. Rec.*, Aug. 1995, pp. 119–124.
[17] D. J. White, D. R. Bowling, and P. L. Overfelt, "Active impedance matching for superdirective supergain HTS antenna arrays," NAWCWPNS Tech. Pub. 8249, China Lake, CA, Apr. 1995.
[18] D. R. Bowling, private communication, 1995.
[19] W. R. Smythe, *Static and Dynamic Electricity*. New York: McGraw-Hill, 1950, pp. 7–10, 547.
[20] F. E. Borgnis and C. H. Papas, "Electromagnetic waveguides and resonators," in *Encyclopedia of Physics*, S. Flugge, Ed. Berlin, Germany: Springer-Verlag, 1958, vol. XVI, pp. 317–318.
[21] H. T. H. Piaggio, *An Elementary Treatise on Differential Equations and Their Applications*. London, U.K.: Bell, 1933, chs. 11, 12.
[22] G. W. Bluman and J. D. Cole, *Similarity Methods for Differential Equations*. New York: Springer-Verlag, 1974, pp. 74–77.
[23] P. Lorraine and D. R. Corson, *Electromagnetic Fields and Waves*. San Francisco, CA: Freeman, 1970, ch. 14.
[24] W. Leighton, *Ordinary Differential Equations*. Belmont, CA: Wadsworth, 1970, chs. 2, 8, 13.

P. L. Overfelt, photograph and biography not available at the time of publication.